Energy Proceedings
Vol 30, 2023
ISSN 2004-2965

Optimization of open refrigerated display cabinet based on different package arrangements

Shengchun Liu[1, 2], Huan Liu[1], Yang Zheng[1], Xueqiang Li[1] Yonghui Guo[1]

1 a Key Laboratory of Refrigeration Technology of Tianjin, Tianjin University of Commerce, Tianjin, 300134, P. R. China

2 Key Laboratory of Efficient Utilization of Low and Medium Grade Energy, Tianjin University, Tianjin, 300350, P. R. China

(Corresponding Author: Xueqiang Li, xqli@tjcu.edu.cn)

ABSTRACT

Open refrigerated display cabinet (ORDC) is widely used in supermarket. It is very convenient for customer to take package. Therefore, the package is not full in ORDC in most time. And the different package arrangement could directly affect ORDC performance. Therefore, this paper optimizes the ORDC and aims to find an optimal structure to meet all different package arrangements. By using the validated model, the windshield and airfoil were employed. Results showed the optimal windshield width, the distance of from evaporator to windshield, and the distance from airfoil structure to shelf edge were 70 mm, 210 mm, and 80 mm, respectively. Under different package arrangements, the average temperature only varied 0.8 °C and the energy consumption 9%. The results obtained in this paper could provide guidance to optimize ORDC.

Keywords: Open refrigerated display cabinet (ORDC), windshield, airfoil structural

NONMENCLATURE

Abbreviations	
COP	Coefficient of performance
DAG	Discharge air grill
ORDC	Open refrigerated display cabinet
PCM	Phase change materials
PBP	Perforated back panel
RAG	Return air grill
Symbols	
α	Constant in regression analysis, gH2O/(m3·°C)
P	Pressure, Pa
P	Energy consumption, (W)
Q	Sensible heat transfer power of evaporator, W
u, v, w	x, y, z direction velocity, m/s
ρ	Density, kg/m^3
μ	Dynamic viscosity, Pa·s
Δω	Difference in moisture content, gH_2O/m^3

1. INTRODUCTION

Open refrigerated display cabinet (ORDC) is widely used in supermarket. It is convenient for customer to take packages [1]. However, since the usage of air curtain in ORDC, the large energy consumption is the key issue. It is affected by many factors, in which the arrangement of package should be also considered.

In the open literatures, the impact of status of package is not fully considered. Most of them optimize ORDC when it was full with package. The structure [5, 6], the air guiding strip [2], and the phase change material (PCM) [3, 4] can be found to improve the ORDC performance. For example, Wu et al. [5] discussed the effect of porosity of the perforated back panel (PBP) (0% - 7%) on average temperature. Result found 3% of porosity of PBP could achieve the minimum average temperature. Li et al. [6] used solid shelves to separate the cabinet into several chambers and send cold air into each chamber. Result showed that maximum temperature uniformity in the cabinet had decreased from 12.1 °C to 1.9 °C. There also have some optimized scenarios in which the ORDC is empty. For example, Chen [7] explored the effect of jet angle of discharge air grill (DAG) on volume entrainment rate. Result found that it was 0.12 m^{3}s^{-1} when jet angle was 17.5°. Similar work can also be found to discuss the impact of jet width [8], jet thickness, and jet length at (discharge air grill) DAG on its performance [9].

During the operation, the package would be taken away by customers. Different package status would affect the performance of ORDC. It is clear that, there is no work regarding this. To bridge the knowledge gap, this paper firstly discusses the impact of package

arrangement on performance. Then the optimization is conducted to meet all different package arrangement. The conclusion obtained in this paper could provide a guidance when the performance optimization of ORDC parameters.

2. MODEL DESCRIPTION AND VALIDATION

2.1 Description of ORDC

Fig. 1 shows the scheme of ORDC. It could provide an effective protection for inner packages and reduce the mixture between inner and ambient air, which mainly includes shelves, DAG, return air grill (RAG), evaporator, fan, PBP. During ORDC operating, the air is cooled down through the evaporator. Then the cold air is divided into two parts: one is transferred through the cold air channel to form the air curtain between DAG and RAG; and the other is used to cool down the packages through the PBP. In the structure, windshield is used to adjust the flow rate for every shelf and the airfoil is to adjust the air curtain, which could reduce the impact of different package arrangements. 7 cases can also be found in Fig. 1, which is used to simulate the different package arrangements. More detailed parameters for ORDC can be found in Table 1.

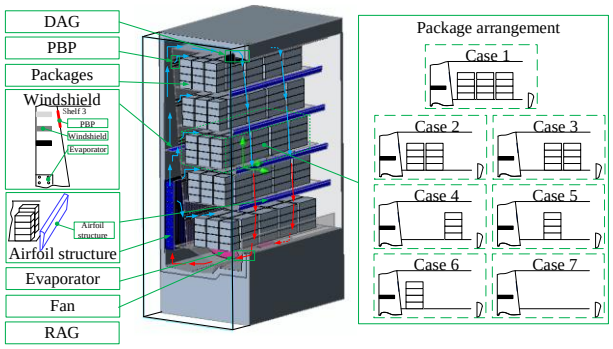

Fig 1 The scheme of ORDC

Table 1 Main parameters of ORDC

Parameters	Value	Step
W×L×H (mm×mm×mm)	770×1310 ×2000	/
Cellular network thickness (mm)	45	/
Porosity of PBP (%)	3	/
Fan model	YZF10-20	/
Number of fans	2	/
Evaporator temperature (°C)	-6	/
Windshield width (mm)	60-100	10
Distance from evaporator to windshield (mm)	200-300	10
Airfoil structure (mm)	40	/
Distance from airfoil to shelf edge	20-100	20
Ambient temperature (°C)	25	/
Humidity (%)	60	/

2.2 Governing equation and boundary conditions

The continuity equation can be found as follows [10]:

$$\frac{\partial u}{\partial x}+\frac{\partial v}{\partial y}+\frac{\partial w}{\partial z}=0 \quad (1)$$

where, u, v and w are the velocity in directions x, y and z, respectively.

Momentum conservation equation is the following:

$$\rho\left(\frac{D\vec{V}}{Dt}\right)=\rho g-\nabla P+\mu\nabla^2\vec{V} \quad (2)$$

where, ρ, t, g, P and μ are density, time, gravitational acceleration, pressure and dynamic viscosity, respectively. Then the momentum equation was solved by k- ε turbulence model.

Energy conservation equation can be found as follows [11]:

$$\frac{\partial(\rho T)}{\partial t}+\frac{\partial(\rho uT)}{\partial x}+\frac{\partial(\rho vT)}{\partial y}+\frac{\partial(\rho wT)}{\partial z}=\frac{\partial}{\partial x}\left(\frac{k}{c_p}\frac{\partial T}{\partial x}\right)+\frac{\partial}{\partial y}\left(\frac{k}{c_p}\frac{\partial T}{\partial x}\right)+\frac{\partial}{\partial z}\left(\frac{k}{c_p}\frac{\partial T}{\partial z}\right) \quad (3)$$

where, T, k and cp are temperature, heat transfer coefficient of the fluid and specific heat capacity, respectively.

In the simulation, the boundary conditions can be found in Table 2.

Table 2 boundary condition of ORDC

Items	Boundary conditions	Values
Calculation zone	W×L×H (mm×mm×mm)	4310×4810×2 895
Ambient	Velocity inlet (m/s)	0.2
	Temperature (°C)	25
	Humidity (%)	60
Fans	Fan flow (m^3/h)	300
Evaporator	Evaporator temperature (°C)	-6
ORDC, packages, floor, and ceiling	Walls	Coupled boundary

2.3 Performance indicators

To evaluate the performance, average temperature and energy consumption are employed.

Average temperature ($\overline{T}$) of ORDC is important for the package storage. It can be calculated as follows

$$\overline{T}=(T_1+T_2+\cdots T_{120})/120 \quad (4)$$

where, $\overline{T}$ represents the average temperature on ORDC, where 120 of measurements are arranged for the whole ORDC.

Energy consumption can evaluate the necessary energy for different operational parameters, which can be calculated as the following [12]:

$$P_{total}=P_{curtain}+P_{cond} \quad (5)$$

where, Ptotal, Pcurtain, and Pcond represent total power of refrigeration system, power consumption to form air

curtain, and power loss due to condensation, respectively.

2.4 Grid independence test

The grid independence test was conducted, as shown in Table 3. Results showed when the grid number was large than 298000, the temperature varied less than 0.4 °C. Therefore, this number was employed.

Table 3 grid independence test

Grid (10^5)	0.85	1.99	2.59	2.98	3.63	4.53	5.36
$\overline{T}$	6.48	5.33	4.98	4.78	4.59	4.53	4.50

2.5 Model validation

The experiment was conducted by using ORDC to validate the proposed model. The experimental test was performed according to ISO 23953. 20 thermocouples were arranged on every shelf; as shown in Fig. 2. Temperatures were recorded every 30 s after the temperatures of ORDC were start. And the temperature data during 21h (75600 s) were analyzed to calculate the average temperature for packages.

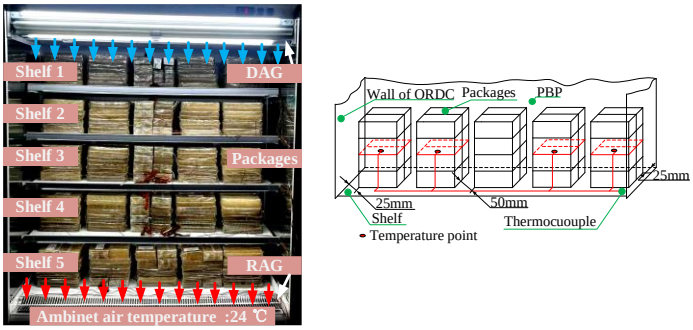

(a) ORDC with full package *(b)Temperature measurements*

Fig. 2 ORDC picture and temperature measurements

The model validation can be found in Fig. 3. Good agreements can be found. As the time going, the average temperature decreased for both experiment and simulation. Since the experiment environment was more complex, the simulation results were always lower than that of experiment. The maximum absolute deviation (0.3 °C) occurred at 21h (75600 s), which was mainly caused by the variation of environment air parameter. Therefore, the model was considered as validated and can be used to predict the performance of ORDC.

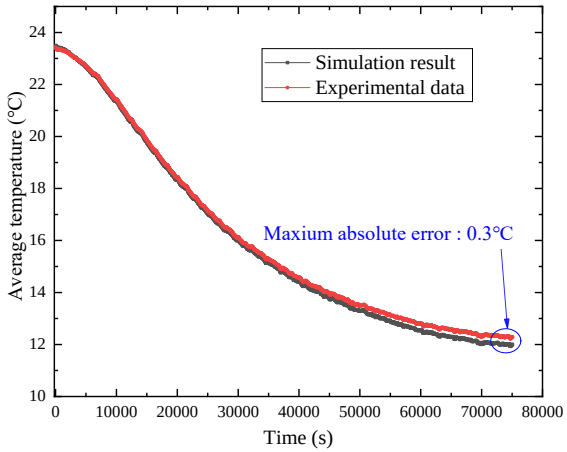

Fig 3 Model validation

3. DISCUSSION

Fig. 4 shows the ORDC performance under different cases without consideration of windshield and airfoil structure. It was clear that, Case 2 and Case 7 had the highest energy consumption and average temperature, respectively; while Case 3 lowest. The difference in average temperature could achieve as high as 1.3 °C and the energy consumption could vary 16%. Therefore, the optimization should be conducted to meet all different cases to improve the ORDC performance.

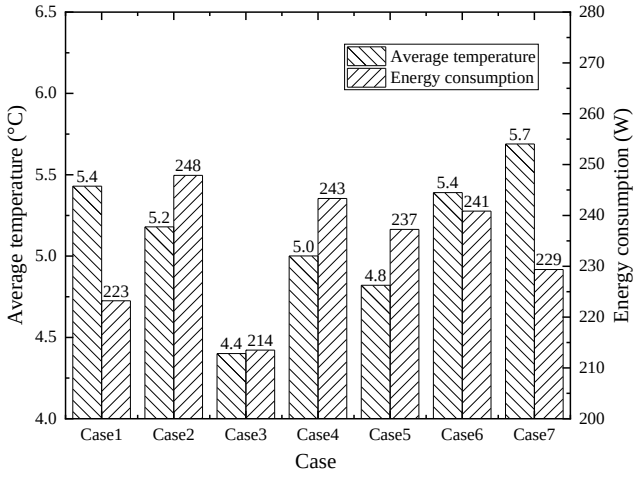

Fig. 4 Impact of different package arrangement

The effect of windshield on ORDC performance can be found in Fig 5, in which the condition of packages was full load and no airfoil structure were used. Apparently, when the windshield width and the distance from evaporator to windshield were 70 mm and 210 mm respectively, the performance of was the best compared with other condition, where the average temperature and energy consumption were only 2.6 °C and 177 W, respectively. When the windshield width was 60 mm, the change trend of energy consumption and average temperature was similar to that of the windshield width of 70 mm, it can be seen a trend of first increased and then decreased. In such condition, with the rise of distance from evaporator to windshield, the flowrate at shelf 4 increased, which was harmful to form air curtain,

whereas, ambient air would invade the inside of the shelves and cause the risk of air average temperature, when the distance from evaporator to windshield was above 270 mm, the flowrate at the shelf 3 and shelf 4 increased, which divided into two parts, reduced the impact of cold air, benefited to cold air returning back to RAG and reduced the inner air average temperature. For windshield width were 80 mm, 90 mm and 100 mm, respectively, the energy consumption and average temperature had been increasing, and the overall value was a high level. This was mainly because the vertical distance between windshield and PBP get smaller and smaller with the windshield width increased, resulted in lots of cold air entered into bottom shelves and broke up the air curtain. Therefore, the optimal windshield width and distance from evaporator to windshield were 70 mm and 210 mm.

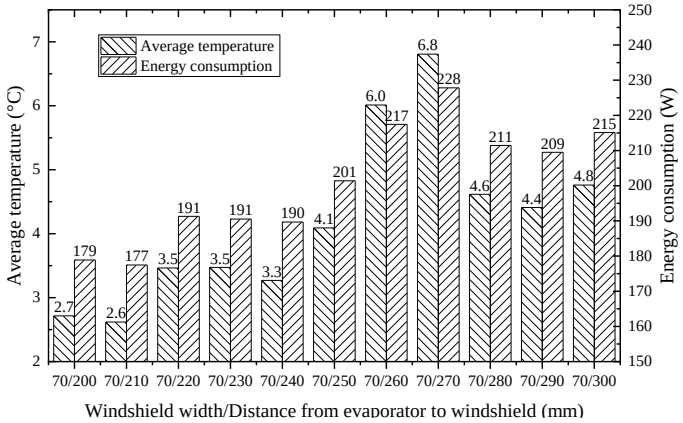

Fig 5 Effect of windshield on ORDC performance

The effect of airfoil structure on ORDC performance can be found in Fig 6, in which the condition of packages was full load, windshield width and the distance from evaporator to windshield were 70 mm and 210 mm. Apparently, the performance of distance from airfoil structure to shelf edge was the best compared with other condition, which the average temperature and energy consumption were only 1.6 °C and 203 W, respectively, indicating the use of airfoil structure would reduce internal air average temperature in a large part in practical conditions. Moreover, it should be note that under the condition that the windshield width and the distance from evaporator to windshield were 70 mm and 210 mm, respectively, the energy consumption increased by 26 W when used airfoil structure compared with not used it. However, compared with other windshield conditions, the average temperature with airfoil structure was about 2.6 °C lower than that without airfoil structure under same energy consumption. This was mainly because the airfoil structure could promote the formation of the air curtain and reduce the internal air average temperature.

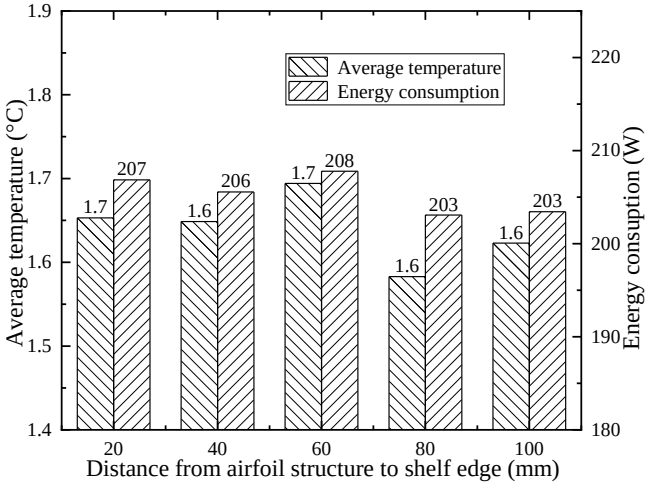

Fig 6 Effect of airfoil structure on ORDC performance

The effect of packages arrangement on ORDC performance can be found in Fig 7. Apparently, the difference in average temperature could achieve as high as 0.8 ° C and the energy consumption could vary 9%. This was due to the windshield and airfoil structure were added to adjust the internal flow distribution, increased the amount of cold air entered the shelf 4 and 5, and made the internal air flow organization more reasonable. Therefore, it showed that when the windshield width and the distance from evaporator to windshield were 70 mm and 210 mm, and the distance from airfoil structure to shelf edge was 80 mm, no matter how the internal number of packages changes, its internal performance change little.

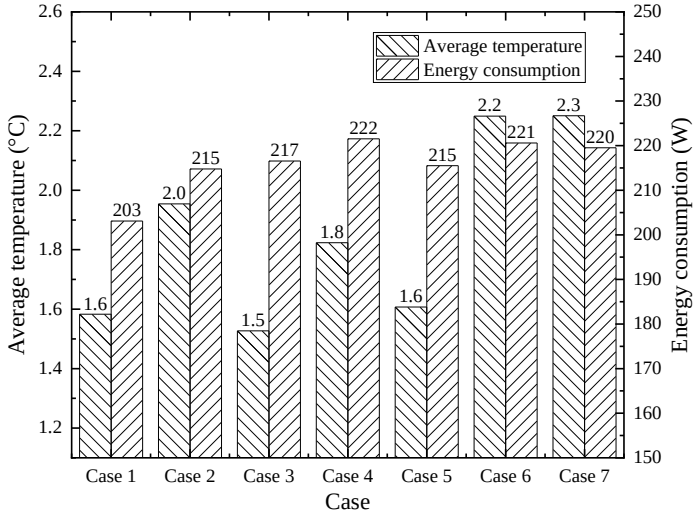

Fig 7 Impact of different package arrangement

4. CONCLUSIONS

The impact of package arrangement on ORDC performance is discussed in this paper. Based on this, the ORDC is optimized to meet all different package arrangements. Through the result, it can be concluded as follows: (1) The average temperature varied as high as 1.3 °C and energy consumption 16% with different package arrangements. (2) The application of windshield

and airfoil could improve ORDC to meet different package arrangements. (3) After optimization, the average temperature varied within 0.8 °C and the energy consumption 9%, compared to 7 cases.

ACKNOWLEDGEMENT

This work is supported by the Science and Technology Program of Tianjin (No. 2021ZD031), and Student's Platform for Innovation and Entrepreneurship Training Program (No. 202210069035). The financial supports are sincerely appreciated.

REFERENCE

[1] Y.G. Chen, X.L. Yuan, Experimental study of the performance of single-band air curtains for a multi-deck refrigerated display cabinet. J Food Eng 2004;69: pp261–267.
https://doi.org/10.1016/j.jfoodeng.2004.08.016

[2] J. Sun, K.M. Tsamos, S.A. Tassou, CFD comparisons of open-type refrigerated display cabinets with/without air guiding strips. Energy Procedia 2017;123: 54–61.
https://doi.org/10.1016/j.egypro.2017.07.284

[3] F.A. Alzuwaid, Y.T. Ge, S.A. Tassou, J. Sun, The novel use of phase change materials in an open type refrigerated display cabinet: A theoretical investigation. Appl Energ 2016;180: 76–85.
https://doi.org/10.1016/j.apenergy.2016.07.088

[4] Y.L. Lu, W.H. Zhang, P. Yuan, M.D. Xue, Z.G. Qu, W.Q. Tao, Experimental study of heat transfer intensification by using a novel combined shelf in food refrigerated display cabinets (Experimental study of a novel cabinets). Appl Therm Eng 2010;30: 85–91.
https://doi.org/10.1016/j.applthermaleng.2008.10.003

[5] X.H. Wu, Z.J. Chang, P. Yuan, Y.L. Lu, Q.Y. Ma, X.M. Yin, The optimization and effect of back panel structure on the performance of refrigerated display cabinet. Food Control 2014;40: 278–285.
https://doi.org 10.1016/j.foodcont.2013.12.009

[6] Z.Q. Li, X.S. Zeng, D. Zhao, G.L. Ding, Schemes and effects on improvement of temperature uniformity inside indirct cooling wine cabinet. Appl Therm Eng 2019;157: 113723.
https://doi.org/10.1016/j.applthermaleng.2019.113723

[7] Y.G. Chen, Parametic evaluation of refrigerated air curtains for thermal insulation. Int J Therm Sci 2009; 48: 1988–1996.
https://doi.org/10.1016/j.ijthermalsci.2009.03.003

[8] L. Cong, Q.H. Yu, G. Qiao, Y.L. Li, Y. L. Ding, Effects of air curtain on temperature distribution in refrigerated vehicles under a hot climate condition. J Therm Sci Eng Appl 2019;11: 061010.
https://doi.org/10.1115/1.4043467

[9] Y.T. Ge, S.A. Tassou, Simulation of the performance of single jet air curtains for vertical refrigerated display cabinets. Appl Therm Eng 2001; 21: 201–219.
https://doi.org/10.1016/S1359-4311(00)00040-5

[10] P.K. Kausthubharam, N. Koorata, Chandrasekaran, Numerical investigation of cooling performance of a novel air-cooled thermal management system for cylindrical Li-ion battery module. Appl Therm Eng 2021;193: 116961.
https://doi.org/10.1016/j.applthermaleng.2021.116961

[11] Y.B. Wang, K. Zhu, Z. Cui, J. Wei, Effects of the location of the inlet and outlet on heat transfer performance in pin fin CPU heat sink. Appl Therm Eng 2019;151: 506–513.
https://doi.org/10.1016/j.applthermaleng.2019.02.030

[12] F. Engdahl, D. Johansson, Optimal supply air temperature with respect to energy use in a variable air volume system. Energ Buildings 2004;36: 205–218.
https://doi.org/10.1016/j.enbuild.2003.09.007